bioRxiv preprint doi: https://doi.org/10.1101/2024.08.31.610645; this version posted September 5, 2024. The copyright holder for this preprint (which was not certified by peer review) is the author/funder, who has granted bioRxiv a license to display the preprint in perpetuity. It is made available under aCC-BY-NC 4.0 International license.

Visual experience-dependent auditory and visual plasticity in the mouse visual cortex

Huub Terra[1*], Leander de Kraker[1], Christiaan N. Levelt[1,2*]

1. Department of Molecular Visual Plasticity, Netherlands Institute for Neuroscience, Amsterdam, Netherlands.

2. Department of Molecular and Cellular Neurobiology, Center for Neurogenomics and Cognitive Research, VU University Amsterdam, Amsterdam, Netherlands.

*Correspondence: (h.terra@nin.knaw.nl or c.levelt@nin.knaw.nl)

bioRxiv preprint doi: https://doi.org/10.1101/2024.08.31.610645; this version posted September 5, 2024. The copyright holder for this preprint (which was not certified by peer review) is the author/funder, who has granted bioRxiv a license to display the preprint in perpetuity. It is made available under aCC-BY-NC 4.0 International license.

ABSTRACT

A lack of early visual experience causes pronounced auditory and visual cross-modal changes. However, the visual cortical region-specific cross-modal organization down to the single neuron level remains unknown. Here we used two-photon calcium imaging in awake mice that were reared in darkness from birth to map auditory and visual responsiveness of single neurons. We targeted neurons in the primary visual cortex (V1) and higher visual cortical areas (HVAs) that resemble the ventral and dorsal stream regions. We found that lateral dorsal stream areas showed a pronounced increase in auditory response strength, even after accounting for tone-induced whisker movement. Strikingly, this was accompanied by a decreased visual drive, measured in number of recruited neurons and response strength, although these visual effects were more widespread across cortical regions. Together, these results provide a comprehensive functional map of auditory and visual cross-modal changes after a lack of early visual experience across the mouse visual cortex. Moreover, our results suggest that a lack of visual drive of dorsal stream regions might provide an opportunity for remaining senses to take over.

bioRxiv preprint doi: https://doi.org/10.1101/2024.08.31.610645; this version posted September 5, 2024. The copyright holder for this preprint (which was not certified by peer review) is the author/funder, who has granted bioRxiv a license to display the preprint in perpetuity. It is made available under aCC-BY-NC 4.0 International license.

INTRODUCTION

In congenitally blind individuals the deprived visual cortex can shift its processing to one of the remaining sensory modalities, such as hearing, through a process called cross-modal plasticity[1–4]. In humans, this audio-visual cross-modal plasticity is accompanied by an increased ability to process sounds, for example improved pitch discrimination[5] or auditory localization[3], possibly attributed to the enhanced processing power auditory information by the visual cortex. In contrast, visual processing is impaired but still present, as seen after restoration of sight in adulthood[6–8]. At the same time, after adult reversal of visual impairments sound-evoked activity in the visual cortex can remain elevated[6,7,9]. This suggests that the cross-modal rewiring after early visual deprivation might remain fixed into adulthood and thereby prevent full recovery of vision. How this is organized across the visual cortex on a single neuron level remains unknown.

The visual cortex contains specialized regions which process different types of sensory information; the dorsal stream regions process movement-related information, the ventral stream regions object-like information and the primary visual cortex (V1) processes simpler features. In humans, these regions have been suggested to be differentially sensitive to early visual experience, where especially the dorsal stream regions seem underdeveloped after loss of early visual experience[10]. In rodents, effects of early visual deprivation on visual processing have also been reported. Dark rearing mice from an early age resulted in lower responsiveness of populations of neurons in dorsal stream-like areas to visual stimuli[11], but increased responsiveness to drifting gratings in V1[12]. Together, this shows that dorsal stream regions are more vulnerable to visual experience. However, whether this also means that single neurons of the dorsal stream region become more responsive to sounds remains unknown.

Animal models, and especially mouse models with their abundant options for cell targeting and manipulation, are essential to understand the cell-type specific changes underlying cross-modal changes after loss of early vision. Genetic to functional cellular changes have been reported in the visual cortex after loss of early vision[13–15]. Layer 2/3 and L4 cells change their genetic identity in V1 after dark rearing from early age[14]. Complete removal of retinal input to V1 by binocular

bioRxiv preprint doi: https://doi.org/10.1101/2024.08.31.610645; this version posted September 5, 2024. The copyright holder for this preprint (which was not certified by peer review) is the author/funder, who has granted bioRxiv a license to display the preprint in perpetuity. It is made available under aCC-BY-NC 4.0 International license.

enucleation even shifts the identity of cell types of V1 towards types in the higher visual cortical regions. Together, this suggests that visual experience is crucial for the formation of the sensory identity of visual cortical regions[15]. Functionally, single neurons of the visual cortex are sparsely responsive to sound, either by being tone activated or suppressed[16], and contribute to audio-visual multisensory integration[17–22]. In animal models, loss of early visual experience can cause visual cortical neurons to become more responsive to sounds[23–25]. While most changes in responsiveness have been reported in V1, increased activation of lateral extrastriate area V2 has also been reported[23]. However, overall information about whether visual experience-dependent changes in auditory responses differ between visual cortical subregions is missing. A complicating factor is that recent studies showed that sound-induced neural activity often appeared to be indirectly caused by sound-induced facial movement instead[26,27]. Thus, a comprehensive study of movement-controlled auditory and visual responses of single neurons after loss of early visual experience across the visual cortex of the mouse is missing. Additionally, whether these responses are reversible remains unknown.

We therefore set out to explore the effect of loss of early visual experience on auditory and visual processing throughout V1 and higher visual cortical areas (HVAs) anteromedial (AM), posteromedial (PM), anterior (A), rostrolateral (RL), anterolateral (AL) and lateromedial (LM). We hypothesized that dorsal stream areas[28,30,31] AM, PM, A, RL and AL would be particularly sensitive to a lack of visual experience and would increase auditory processing and decrease visual processing. Visual experience was manipulated by dark rearing mice from birth. In awake, head-fixed and freely running mice, functional auditory and visual changes at the cellular level were recorded using calcium imaging under a two-photon (2P) microscope in response to pure-tones and moving-grating stimuli. Recordings were targeted to V1 and the combined HVAs: AM/PM (medial dorsal stream), A/RL/AL (lateral dorsal stream) and LM (ventral stream). For auditory stimuli we corrected for the sound-induced arousal effect using video monitoring and face movement analysis. We found that a loss of visual experience has a pronounced effect on single neurons in HVAs, especially the dorsal stream regions, with an increase in auditory processing and a decrease in visual processing. This study provides the first comprehensive mapping of functional auditory and visual cross-modal changes after loss of early

bioRxiv preprint doi: https://doi.org/10.1101/2024.08.31.610645; this version posted September 5, 2024. The copyright holder for this preprint (which was not certified by peer review) is the author/funder, who has granted bioRxiv a license to display the preprint in perpetuity. It is made available under aCC-BY-NC 4.0 International license.

visual experience and can contribute to the cellular level understanding of the cross-modal changes after early loss of vision.

RESULTS

Dark rearing increases responsiveness of neurons in anterior higher visual cortical areas to pure tones.

To test the effect of loss of early visual experience on auditory processing of single neurons across visual cortical regions we presented pure-tone stimuli to naive mice. One group of mice was reared in absolute darkness from birth and therefore lacked any visual experience and a second group was reared in normal light/dark conditions (**Fig. 1A**). Adult mice were first placed under a wide-field macroscope to determine the location of visual cortical areas using population receptive field mapping and the Allen Brain reference atlas (**Fig. 1B**)[29,30,32]. Activity of single layer 2/3 neurons was recorded using 2P calcium imaging in awake, head-fixed mice that were free to run while pure tones were presented from a single speaker in front of mouse (**Fig. 1C**). Stimuli were presented in darkness while facial movement and run speed were recorded under infrared light.

Recent work showed that sound-induced activity of V1 neurons is predominantly correlated to facial movement instead of sound itself[26,27,33]. Especially movement of the whisker pad had a high predictive value for neuronal activity[27]. Temporally, in neural activity the motor-related component was strongest after about 200 to 300 ms whereas the auditory component was strongest before that time[26]. As expected, we found that pure tones elicit whisker movement (**Fig. S1A and B**). Both tone onset and offset evoked whisker movement (**Fig. S1B and D**). Normally reared and dark reared animals showed frequency- and intensity-dependent whisker movement (**Fig. S1C**). Tones with a higher intensity (**Fig. S1D**) and around the peak frequency sensitivity in mouse hearing of around 6 kHz[34] (**Fig. S1E**) induced the strongest whisker movement. No effect of rearing condition was observed. To minimize arousal-related components in tone-induced neuronal activity we: 1) removed all trials with Z-scored whisker movement energy above two, 2) improved the temporal resolution of our fluorescence signal by estimating spike times with a spike deconvolution algorithm[35] and restricted our analysis to approximately the first 250 ms after tone onset or offset.

bioRxiv preprint doi: https://doi.org/10.1101/2024.08.31.610645; this version posted September 5, 2024. The copyright holder for this preprint (which was not certified by peer review) is the author/funder, who has granted bioRxiv a license to display the preprint in perpetuity. It is made available under aCC-BY-NC 4.0 International license.

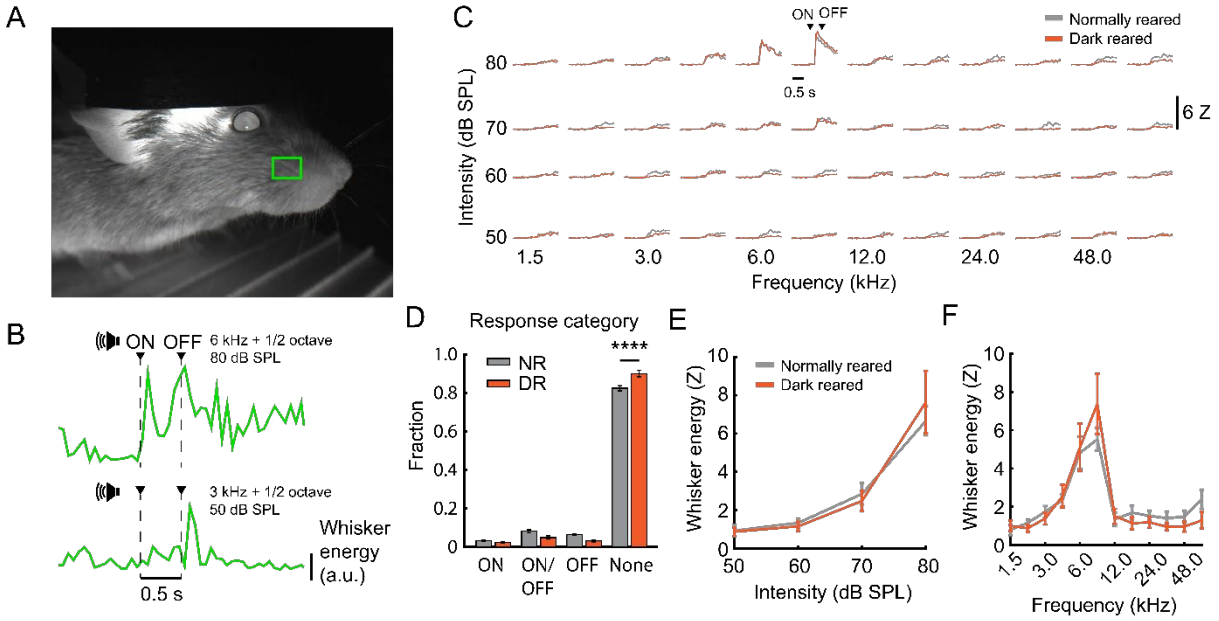

Supplementary figure 1. Tone intensity-dependent and frequency-dependent increase in whisker movement.

(A) Example movie image from the face of a mouse in darkness with only infrared light. Green square, whisker region.
(B) Example trials with whisker energy (from the green square in (A)) in response to a tone with an ON/OFF response (top) and OFF response (bottom).
(C) Session-averaged frequency response area of the whisker energy. Whisker energy is z-scored to 1-0 s before tone onset.
(D) Fraction of response categories. ON, average whisker energy (z-scored) between 0 to 0.5 s above 2 during this period only. ON/OFF, average whisker energy (z-scored) between 0 s to 0.5 s and 0.5 s to 1.0 s above 2. OFF, average whisker energy (Z-scored) between 0.5 s to 1.0 s above 2 during this period only, None, average whisker energy (z-scored) between 0 s to 0.5 s or 0.5 s to 1.0 s below 2. Two-way ANOVA with Dunn-Sidak multiple comparison correction, Category x rearing, $F_{(3,168)} = 15.42$, $p < 0.0001$, NR None vs DR None, $p < 0.0001$. Data is session averaged over trials. Normally reared, 19 sessions, Dark reared, 25 sessions.
(E) Whisker energy (z-scored) per tone intensity. Tone intensities were used across the strongest frequency response. Two-way repeated measures ANOVA. Intensity, $F_{(2.249,88.33)} = 23.49$, $p < 0.0001$, rearing, $F_{(1,40)} = 3.273e-005$, $p = 0.9955$, intensity x rearing, $F_{(11,432)} = 1.169$, $p = 0.3063$.
(F) Whisker energy (z-scored) per frequency. Tone frequencies were used across the strongest intensity response. Frequency, $F_{(1.419,50.14)} = 33.50$, $p < 0.0001$, rearing, $F_{(1,36)} = 0.2513$, $p = 0.6192$, frequency x rearing, $F_{(3,106)} = 0.7808$, $p = 0.5072$.

We recorded the frequency response areas (FRA) of neurons and observed that pure tones can activate and inhibit neurons in the visual cortex (**Fig. 1E**). Both tone onset and offset drove changes in neuronal activity in normally reared and dark animals throughout the visual cortical regions AM/PM, A/RL/AL, LM and V1 (**Fig. 1F**). Neurons in all cortical regions and between rearing conditions showed similar fractions of tone-induced response types (activation, inhibition, both activation and inhibition or no response) in their FRA (**Fig. 1G**). However, dark rearing resulted in a higher tone-induced response amplitude of neurons in the A/RL/AL region at their best frequency (BF, tone with strongest response), but not in other regions (**Fig. 1H**). Further analysis showed no effect of rearing and cortical region on the distribution of best frequencies (**Fig. 1I**) or on frequency selectivity, measured as receptive field sum (RFS)[36] (**Fig. 1J**). Together, this shows that a loss of early visual experience by dark rearing specifically increases the response strength of single neurons to pure tones in lateral dorsal stream HVAs.

bioRxiv preprint doi: https://doi.org/10.1101/2024.08.31.610645; this version posted September 5, 2024. The copyright holder for this preprint (which was not certified by peer review) is the author/funder, who has granted bioRxiv a license to display the preprint in perpetuity. It is made available under aCC-BY-NC 4.0 International license.

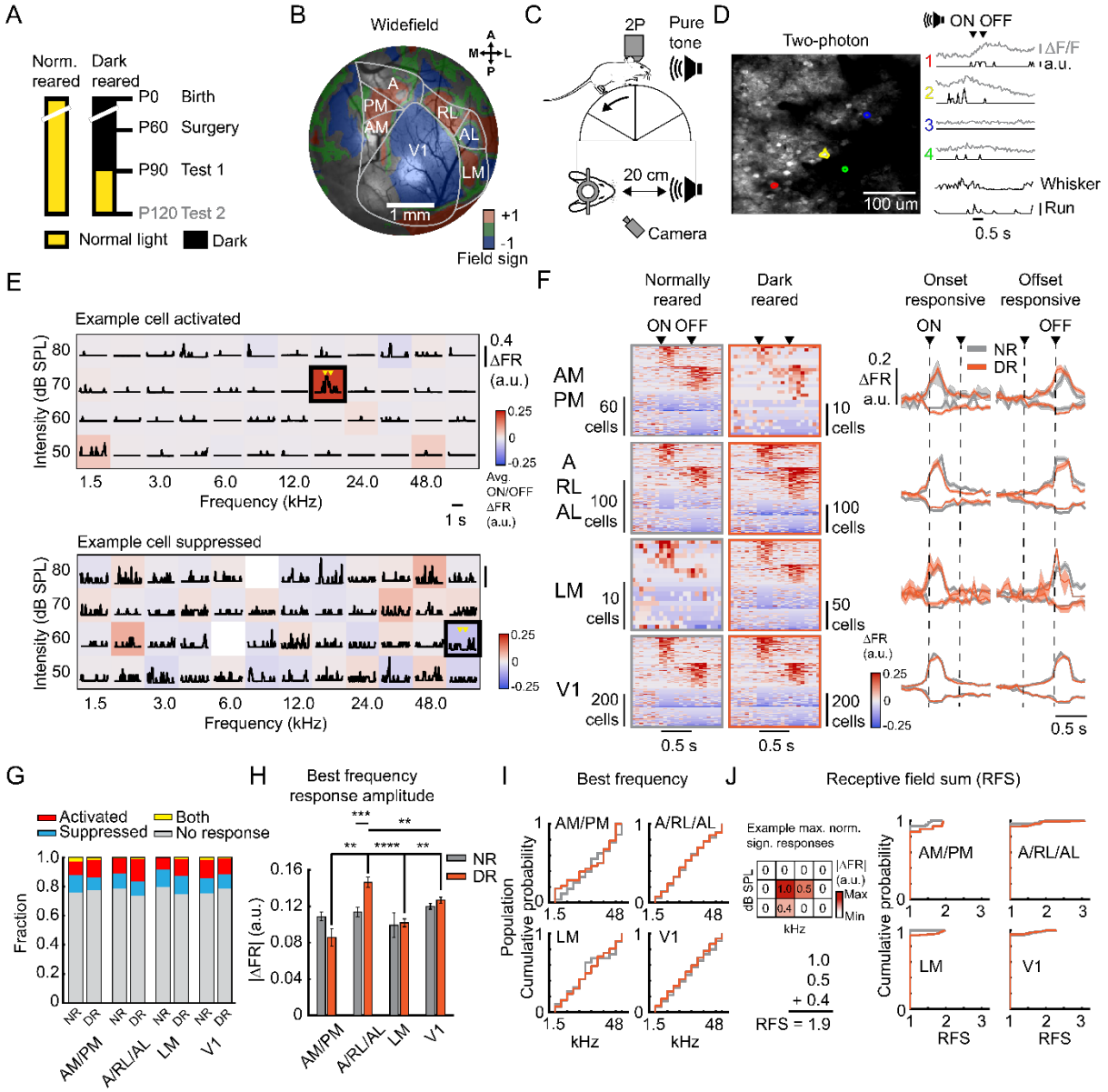

Figure 1. Dark rearing increases responsiveness of neurons in anterior higher visual cortical areas to pure tones.

(A) Experimental groups and timeline.

(B) Example widefield epifluorescence microscopy field of view overlayed with a field sign map and the Allen Brain institute reference atlas.

(C) Schematic of the 2P microscope experimental setup for presentation of pure tone stimuli. Tones are presented for 0.5 s at 12 frequencies ranging from 1.5 kHz to 48 kHz and half-an-octave step with half-an-octave step in between and at 4 intensity levels between 50 and 80 dB sound pressure level (SPL) with 10 dB SPL steps with 2-4 s in between stimuli. Facial movement is recorded using an infrared camera under infrared background light.

(D) Left, example 2P microscopy field of view of the visual cortex with GCaMP8m-expressing cells. Right, Example responses of four cells to a pure tone sound (12 kHz and half-an-octave step at 70 dB SPL). Grey traces, calcium fluorescence (ΔF/F), black traces below grey traces, deconvolved spikes (a.u., bar = 1 a.u.), black traces, whisker energy and run speed (bar = 0.1 cm/s), arrows indicate tone onset and offset.

(E) Example frequency response areas of a cell excited (top) and inhibited (bottom) by pure tones. Traces indicated baseline-corrected mean response over trials in a.u (ΔFR). Raster plot, trial-averaged ΔFR during 0-0.2s after tone onset or offset. Empty slots indicate removed tones due to having less than 8 trials left over after removal of whisker-movement trials. Box indicates strongest significant response to a tone, i.e., best frequency.

(F) Significant responses to pure tones. Per cell the best frequency response is displayed. Left, Plot sorted on response amplitude and response category (tone onset or offset). Right, mean responses over cells that respond strongest with excitation (top), inhibition (bottom), to tone onset (left) and offset (right),

(G) Fraction of response types. Fisher's exact test, $p > 0.05$.

(H) Response amplitude (absolute ΔFR) at the best frequency for tone-responsive neurons. Two-way repeated measures ANOVA with Tukey's multiple comparison's test between groups and within groups, Rearing, $F_{(1, 1912)} = 0.05311$, $p = 0.04662$, Cortical region, $F_{(3, 1912)} = 6.582$, $p < 0.0002$, Interaction, $F_{(3, 1912)} = 4.702$, $p < 0.0028$, n = 19 – 550 cells per group from n = 3-6 mice per group.

(I) Cumulative probability function of best frequencies over all tone-responsive neurons. Mann-Whitney U test, $p > 0.05$.

(J) Receptive field sum (RFS). Left, illustrative schematic of RFS calculation. Right, Cumulative probability function of the RFS of all tone-responsive neurons. Mann-Whitney U test, $p > 0.05$.

bioRxiv preprint doi: https://doi.org/10.1101/2024.08.31.610645; this version posted September 5, 2024. The copyright holder for this preprint (which was not certified by peer review) is the author/funder, who has granted bioRxiv a license to display the preprint in perpetuity. It is made available under aCC-BY-NC 4.0 International license.

Dark rearing decreases responsiveness of neurons in anterior higher visual cortical areas and V1 to drifting gratings.

The specific increase of auditory processing in A/RL/AL visual cortical regions after loss of early visual experience could suggest that this region is especially vulnerable to a lack of early visual experience. We therefore tested if single neuron responses to visual stimuli would correspondingly decrease after dark rearing. To this end, the same normally reared and dark reared mice were also shown full-field drifting gratings at different directions and contrasts (**Fig. 2A**) while neuronal activity was measured using 2P calcium imaging (**Fig. 2B**). As expected, we observed neurons responding to drifting gratings, often with a clear preference to a certain direction and contrast (**Fig. 2C**). Both normally reared and dark reared animals had neurons with responses to drifting gratings across the visual cortical regions (**Fig. 2D**), mainly of the activated type (**Fig. 2E**). In the A/RL/AL, LM and V1 region there was a decrease in the overall fraction of responsive neurons after dark rearing (**Fig. 2E**). Additionally, we observed a decrease in the response amplitude to the preferred stimulus after dark rearing in both the AM/MP and A/RL/AL regions (**Fig. 2F**). Ad-hoc two-way ANOVAs with Bonferroni correction targeted to A/RL/AL vs LM and A/RL/AL vs V1 showed that the decreased response amplitude was greater for A/RL/AL compared to V1 (rearing x area, $F_{(1, 2918)} = 5.529$, $p = 0.0376$) but not for A/RL/AL compared to LM (rearing x area, $F_{(1, 1161)} = 2.613$, $p = 0.2126$). Similar analysis for AM/PM vs LM (rearing x area, $F_{(1, 815)} = 3.120$, $p = 0.1574$) and AM/PM vs V1 (rearing x area, $F_{(1, 2572)} = 4.456$, $p = 0.0698$) were non-significant.

In conclusion, a lack of early visual experience reduced the responsiveness of the visual cortex to drifting gratings. While the fraction of responsive neurons decreased in primary and HVAs, only dorsal stream regions showed reduced response amplitude.

bioRxiv preprint doi: https://doi.org/10.1101/2024.08.31.610645; this version posted September 5, 2024. The copyright holder for this preprint (which was not certified by peer review) is the author/funder, who has granted bioRxiv a license to display the preprint in perpetuity. It is made available under aCC-BY-NC 4.0 International license.

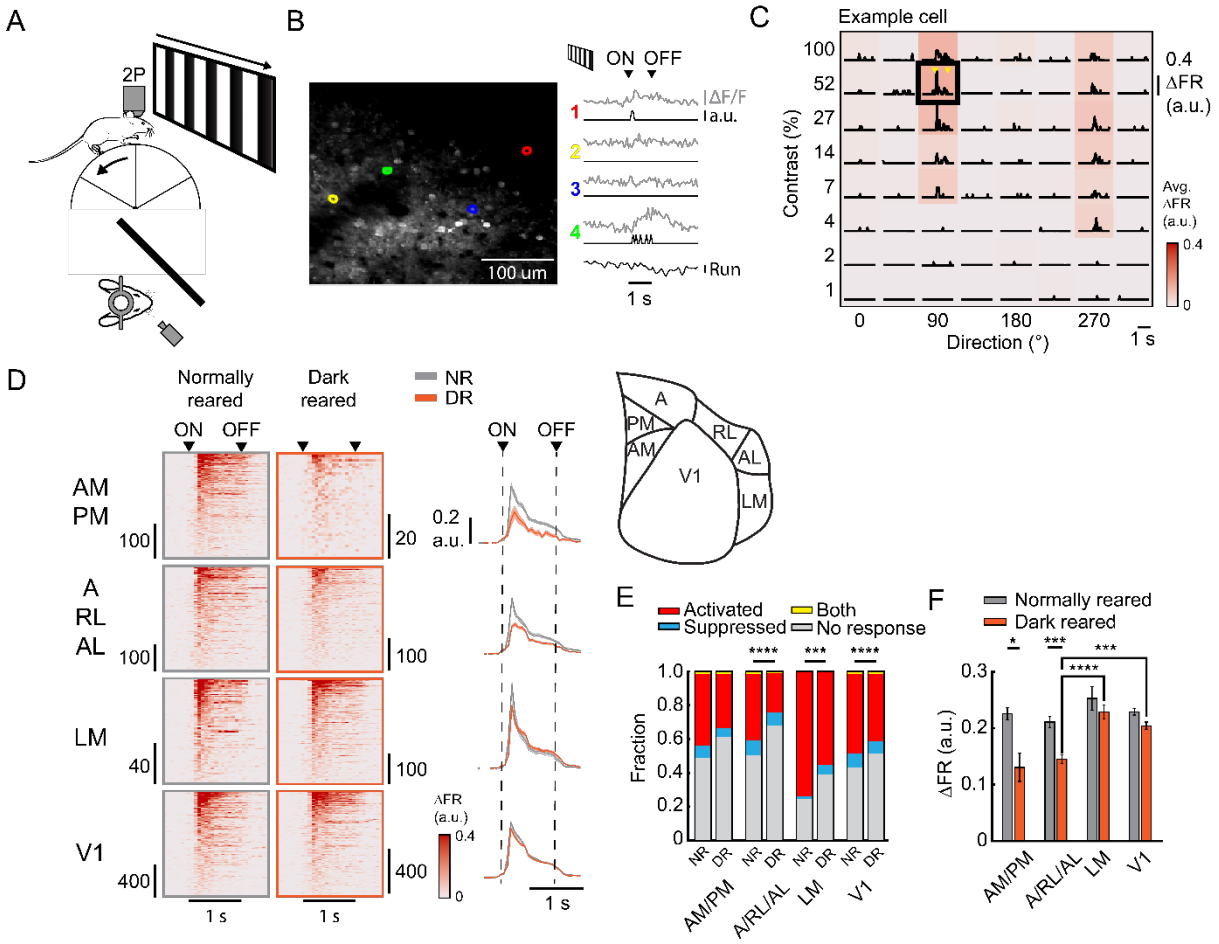

Figure 2. Dark rearing decreases responsiveness of anterior higher visual cortical and V1 neurons to drifting gratings.

(A) Schematic of the 2P microscopy experimental setup for presentation of moving grating stimuli. Gratings are presented for 1 s at 8 directions with 45˚ in between and at 8 contrast levels between 1 and 100% contrast with 3 s in between stimuli and 15 repetitions per stimuli.
(B) Left, example 2P microscopy field of view of the visual cortex with GCaMP8m-expressing cells. Right, Example responses of four cells to a drifting grating. Grey traces, calcium fluorescence (ΔF/F), black traces below grey traces, deconvolved spikes (a.u., bar = 1 a.u.), black traces, run speed (bar = 0.1 cm/s), arrows indicate tone onset and offset.
(C) Lines, example trial-averaged ΔFR to drifting gratings. colormap, trial-averaged ΔFR during 0-0.5 s after stimulus onset.
(D) Activated cells to moving gratings. Per cell the strongest response is displayed. Left, Plot sorted on response amplitude. Right, mean responses over cells,
(E) Fraction of response types. Fisher's exact test, NR x DR, AM/PM, p = 0.5490, A/RL/AL, p = 0.0001, LM, p = 0.0001, V1, p = 0.0001.
(F) Response amplitude (ΔFR) at the preferred stimulus for drifting-grating responsive neurons Two-way repeated measures ANOVA with Tukey's multiple comparison's test between groups and within groups, Rearing, $F_{(1, 3733)} = 24.36$, $p = 0.0001$, Cortical region, $F_{(3, 3733)} = 10.41$, $p < 0.0001$, Interaction, $F_{(3, 3733)} = 3.085$, $p < 0.0262$, n = 19 – 550 cells per group from n = 3-6 mice per group.

Dark rearing induces a shift in auditory and visual processing at the neuronal population level.

Next, we assessed whether changes in auditory and visual response strength also had consequences for processing of auditory and visual information on a population level. We trained a linear discriminant classifier to predict sound frequency and intensity (**Fig. 3A**), or grating direction and contrast (**Fig. 3D**) based on the change in

bioRxiv preprint doi: https://doi.org/10.1101/2024.08.31.610645; this version posted September 5, 2024. The copyright holder for this preprint (which was not certified by peer review) is the author/funder, who has granted bioRxiv a license to display the preprint in perpetuity. It is made available under aCC-BY-NC 4.0 International license.

activity across the population of neurons. We chose a less stringent approach to deal with possible effects of whisker movement as confound for neural activity: 1) we used the $\Delta F/F_0$ as neuronal activity, 2) Linear regression was used to filter out whisker movement and running speed from the $\Delta F/F_0$ signal.

Normally reared animals showed a modest but significantly increased decoding accuracy of sound frequency compared to chance in AM/PM and A/RL/AL. Dark rearing further increased frequency decoding accuracy only in A/RL/AL (**Fig. 3B**). Sound intensity was decoded above chance in AM/PM, A/RL/AL and V1 in normally reared animals and dark rearing further increased intensity decoding accuracy in AM/PM, A/RL/AL and LM (**Fig. 3C**).

Grating direction and contrast decoding accuracy was above chance across brain regions and rearing condition (**Fig. 3E and F**). Dark rearing decreased decoding accuracy for grating direction in AM/PM and A/RL/AL but increased decoding accuracy for LM (**Fig. 3E**). Similarly, dark rearing decreased decoding accuracy for contrast in AM/PM and A/RL/AL but surprisingly an increased decoding accuracy for both LM and V1 (**Fig. 3F**).

Together, these results indicate that on the neuronal population level sound auditory information increases after loss of early visual experience, especially in HVAs. In contrast, visual information decreases in medial and dorsal higher visual cortical regions after dark rearing but increases in LM and V1.

bioRxiv preprint doi: https://doi.org/10.1101/2024.08.31.610645; this version posted September 5, 2024. The copyright holder for this preprint (which was not certified by peer review) is the author/funder, who has granted bioRxiv a license to display the preprint in perpetuity. It is made available under aCC-BY-NC 4.0 International license.

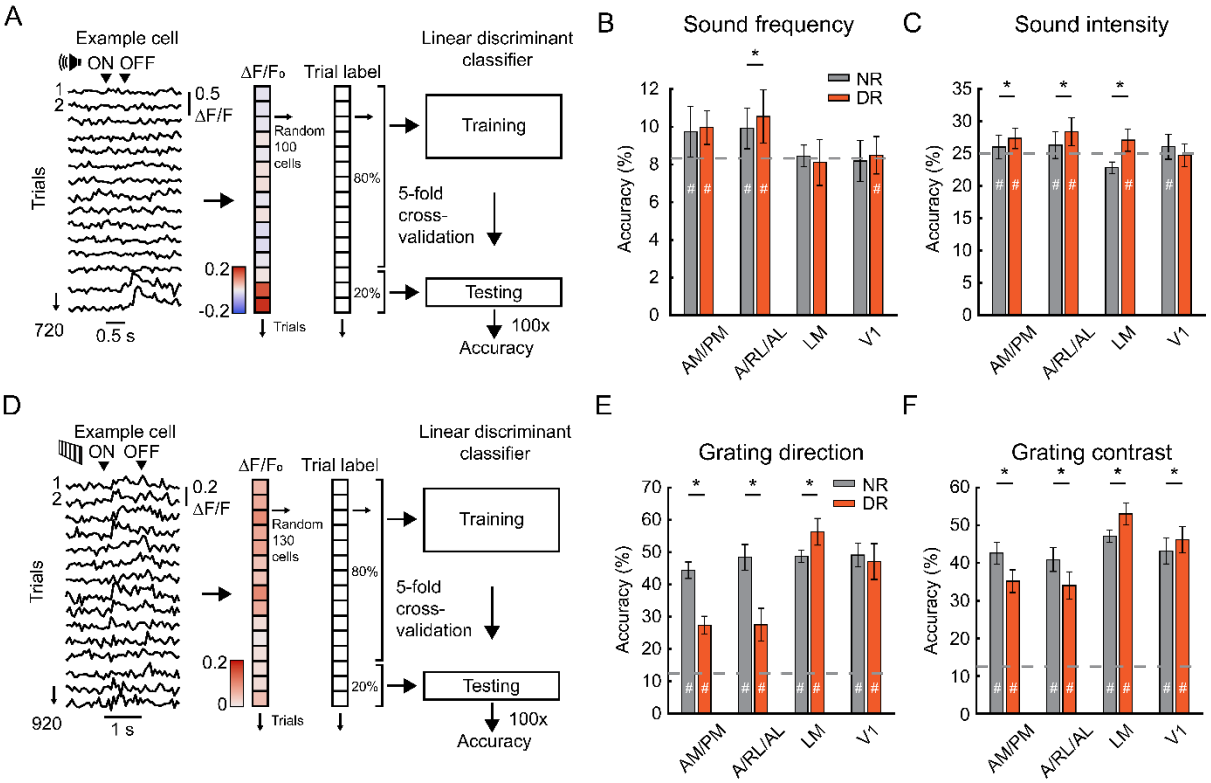

Figure 3. Dark rearing induces a shift in auditory and visual processing at the neuronal population level.

(A) Schematic of the linear discriminant classifier for pure tones. To train the model: 1) all trials with ΔF/F signal are used, 2) the baseline corrected $\Delta F/F_0$ values are calculated and then the running and whisker movement activity is linearly regressed out. 3) a trial X neuron matrix with $\Delta F/F_0$ values and trials labels (frequency, intensity, direction or contrast) is made where the number of neurons is set at the minimum number found across groups, 4) using this data a linear discriminant classifier is trained to predict trial labels. This model is validated using 5-fold cross-validation. The complete procedure is repeated 100 times with randomly picked neurons to produce a distribution of accuracies.
(B) Decoding accuracies for sound frequency.
(C) Decoding accuracies for sound intensity.
(D) Schematic of the linear discriminant classifier for drifting gratings, like (A).
(E) Decoding accuracies for drifting grating direction.
(F) Decoding accuracies for drifting grating contrast.

(B, C, E and F) Permutation tests with Bonferroni correction, #, $p < 0.05$ accuracy vs. chance, *, $p < 0.05$ normally reared vs dark reared.

DISCUSSION

Here we describe cortical region-specific effects of a lack of early visual experience on auditory and visual processing down to the single neuron level. A lack of early visual experience increased sound-evoked response strength specifically in neurons of the dorsal stream areas A/RL/AL. This dorsal stream-specific effect was accompanied by a pronounced decreased processing of visual stimuli by neurons in A/RL/AL as well, although these effects were more widespread across cortical regions.

In both humans and mice, dorsal stream regions and associated functions are particularly sensitive during early development[10,11,37]. In humans, developmental

bioRxiv preprint doi: https://doi.org/10.1101/2024.08.31.610645; this version posted September 5, 2024. The copyright holder for this preprint (which was not certified by peer review) is the author/funder, who has granted bioRxiv a license to display the preprint in perpetuity. It is made available under aCC-BY-NC 4.0 International license.

disorders such as Williams syndrome, autism spectrum disorder and cerebral palsy are associated with impaired performance on tasks involving visual motion processing[10]. Individuals with early onset blindness also show pronounced deficits in motion processing regions such as middle temporal gyrus, middle occipital gyrus and right cuneus[3,38]. In mice, populations of neurons in dorsal stream regions, especially AM/PM and AL, develop visual tuning later after eye opening and become less responsive to visual stimuli after dark rearing compared to ventral stream regions[11]. This had led to the hypothesis that V1 input to dorsal stream regions compared to ventral stream regions is more dependent on early visual experience[11]. We expand on this work by showing that fewer neurons in dorsal stream regions AM/PM and A/RL/AL are recruited by drifting gratings and become less responsive to visual stimuli after dark rearing. Importantly, we find that these regions also become more responsive to auditory stimuli. Our results therefore provide support for the 'dorsal vulnerability hypothesis' and further suggest that the reduced visual input provides opportunity for auditory inputs to dorsal regions to strengthen.

Recently, sound-evoked activity in the visual cortex has been suggested to be caused indirectly by facial movement instead[39]. While our results indeed find a strong influence of sound on facial movement we do observe sound-evoked activity in single neurons after removing sound-induced whisker movement trials and restricting our analysis windows to periods where more pure auditory activity has been observed. Our results thus support the idea that visual cortical neurons can be activated by sound directly[26] possibly contributing to audiovisual multisensory integration.

The source of increased auditory response strength after dark rearing is still unknown. One hypothesis is that exuberant axons from the auditory cortex that are laid out at birth are not pruned away under the influence of feedforward visual input and remain in place into adulthood[40]. This is supported by anatomical tracing studies in animals[41,42] and human fMRI studies[43]. However, there is also anatomical evidence that auditory subcortical input might drive the visual cortex after lack of early visual experience[25,42,44]. Future experiments using functional imaging targeted to the dorsal stream neurons in combination with auditory cortical or thalamic silencing might provide a clear answer.

bioRxiv preprint doi: https://doi.org/10.1101/2024.08.31.610645; this version posted September 5, 2024. The copyright holder for this preprint (which was not certified by peer review) is the author/funder, who has granted bioRxiv a license to display the preprint in perpetuity. It is made available under aCC-BY-NC 4.0 International license.

In summary, a lack of early visual experience increases auditory and decreases visual processing in the mouse visual cortex, particularly in the dorsal stream. This could enhance dorsal stream-specific auditory processing but hamper restoration of visual tuning in adulthood.

MATERIALS AND METHODS

Animals

All experiments were approved by the institutional animal care and use committee of the Royal Netherlands Academy of Arts and Sciences under Central Committee Animal experiments (CCD) license AVD80100202215934, Academy of Arts and Sciences. We used X male and X female mice in the dark reared group and X male and X female mice in the normally reared group. All mice were F1 offspring from female CBA/JRj (Janvier labs, https://janvier-labs.com/) crossed to male Vipr2-Cre$^{-/-}$ (Jackson Laboratories, https://www.jaxmice.jax.org/, strain 031332[45]. Mice were group housed before surgery. After surgery they were either individually or group housed with *ad libitum* access to food and water under a 12-hour reversed day/night cycle or constant darkness. All mice had access to a running wheel in their home cage. Extra care was taken to ensure dark reared animals remained in absolute darkness up until the first recording. Daily health checks and habituation to the recording setup were done under infrared light (850nm) using custom infrared binoculars. During surgery the eyes were covered using custom light-protective caps. All experiments were performed in the dark phase of normally reared animals.

Viral injection and cranial window surgery

Mice were anesthetized with Isoflurane (5% induction, 1.5 - 2% maintenance in oxygen), body temperature was maintained at a stable 37 ˚C with a euthermic pad and the eyes were covered with light-protective caps filled with Ophtosan eye ointment to prevent them from drying. Metacam (5 mg/kg *s.c.*), Temgesic (0.1 mg/kg *s.c.*), Xylocaine gel (on periost) and Rymadil (0.06 mg/mL, post-operative day 1 to 3 in drinking water) were provided for analgesia and Dexamethason (4-8 mg/kg *s.c.*) for anti-inflammation and to reduce brain swelling. First, the skin and periosteum were removed above the skull. Then, eight holes were drilled in the skull spread

bioRxiv preprint doi: https://doi.org/10.1101/2024.08.31.610645; this version posted September 5, 2024. The copyright holder for this preprint (which was not certified by peer review) is the author/funder, who has granted bioRxiv a license to display the preprint in perpetuity. It is made available under aCC-BY-NC 4.0 International license.

across the visual cortex using a dental drill. A mixture (1:1) of AAV1-hDlx-dlox-mCyRFP1(rev)-dlox (0.67 x 10^{12} titer, VVF Zurich, v313-1) and AAV9-CaMKIIα-jGCaMP8m (0.67 x 10^{12} titer, VVF Zurich, v630-9)[46] was injected at 400 and 200 µm below cortical surface across 8 injections of 9.2 nL at 46nL/s. A craniotomy was drilled above the visual cortex and a cranial window (4+4+5mm diameter stacked cover slips) was carefully lowered in the craniotomy. The window and a custom metal head ring were attached to the skull using dental cement. Mice were allowed to recover from surgery for a minimum of one week after which they were habituated to head fixation in the recording setup until they comfortably started running.

Wide-field calcium imaging

Population receptive field mapping and field sign analysis using the wide-field macroscope was done as described before[29]. In short, the complete 4 mm diameter window was imaged using a wide-field fluorescence macroscope (Axio Zoom.V16 Zeiss/Caenotec-Prof. Ralf Schnabel). Images were captured by a high-speed sCMOS camera (pro.edge 5.5) at 20 Hz, 1600 x 1600 pixels with 50 ms exposure time and recorded with Encephalos software (Caenotec-Prof. Ralf Schnabel) after which they were down sampled to 800 x 800 pixels for analysis.

Two-photon calcium imaging

Two-photon calcium imaging was performed on a 2P microscope (Neurolabware) equipped with a Ti-sapphire laser (Mai-Tai 'Deepsee', Spectraphysics) running at 920 nm, using 16x, 0.8 NA water immersion objective (Nikon) at 1.0x to 1.6x digital zoom. Imaging was controlled by Scanbox software (Neurolabware) running on Matlab at a frame rate of approximately 15.5 Hz. Mice were head fixed and free to run on a wheel. Running speed was recorded using a rotary encoder running on Arduino and processed in Matlab.

Visual stimuli

Wide-field calcium imaging

Mice were positioned at the centre, 14 cm away, from a 122 x 68 cm LCD screen (iiyama LE5564S-B1, 1920 x 1280 pixels at 60 Hz refresh rate) covering a 144° x 86° field-of-view. Stimuli were created and presented using COGENT (developed by John Romaya at the LON at the Wellcome Department of Imaging Neuroscience)

bioRxiv preprint doi: https://doi.org/10.1101/2024.08.31.610645; this version posted September 5, 2024. The copyright holder for this preprint (which was not certified by peer review) is the author/funder, who has granted bioRxiv a license to display the preprint in perpetuity. It is made available under aCC-BY-NC 4.0 International license.

together with Matlab (Mathworks). Stimuli consisted of eccentricity-corrected angled bars at 0°, 45°, 90° or 135° with 10° in diameter of a checkerboard pattern on a grey background (20 cd/m2). A total of 58 stimuli were pseudo-randomly presented 10 times for 0.5 s with an inter-trial-interval consisting of a grey screen (20cd/m^2) for 3.6 s. Images were smoothed using a Gaussian filter with two pixels standard deviation and stored per trial. Population receptive field mapping and field sign analysis was done as described as before[29,30].

Two-photon calcium imaging

Mice were positioned at the centre, 15 cm away, from a 24 inch gamma-corrected HD LED monitor (1920 x 10870 pixels at 60 Hz refresh rate) covering a 120° x 90° field-of-view. Stimuli were created and presented using OpenGl and Psychophysics Toolbox 3 in Matlab. Visual stimuli consisted of eccentricity-corrected full-field sinusoidal drifting gratings at a direction of 0°, 45°, 90°, 135°, 180°, 225°, 270° or 315° at 8 different contrasts logarithmically spaced between 1% and 100% ("logspace(0,2,8)" in Matlab). Each combination of direction x contrast was pseudo randomly presented for 1 s (0.05 cpd at temporal frequency of 1 Hz) with an inter-trial-interval of 2 s where a mean luminance grey screen was presented, this was repeated 15 times.

Auditory stimuli

For 2P calcium imaging a single ultrasound speaker (Batsound, L400 Ultrasound speaker) was positioned at the level of the mouse at 20 cm distance. For measuring frequency response areas pure-tone stimuli were presented and created using Psychophysics Toolbox 3 and Matlab. Pure-tone stimuli were presented in open field at 12 frequencies between 1.5 kHz to 48 kHz and half-an-octave step with half-octave-step in between and at an intensity of 50, 60, 70 and 80 dB sound pressure level (dB SPL) at 192 kHz with 24 bits using the Terratec Aurean Xfire 8.0 HD external soundcard. Peak intensity levels of background noise were measured around 40 dB SPL. Pure-tone stimuli were presented in pseudorandom order for 0.5 s (including a 5 ms cosine-squared rise/decay time) with 2 to 3 s random inter-trial-

bioRxiv preprint doi: https://doi.org/10.1101/2024.08.31.610645; this version posted September 5, 2024. The copyright holder for this preprint (which was not certified by peer review) is the author/funder, who has granted bioRxiv a license to display the preprint in perpetuity. It is made available under aCC-BY-NC 4.0 International license.

interval in between, this was repeated 15 times. Sound intensities were calibrated using a condenser ultrasound microphone (Avisoft-Bioacoustics CM16/CMPA) placed at the position of the pinnae, in combination with the UltraSoundGate 116Hb recording interface and Avisoft-RECORDER USGH software.

Video tracking and whisker energy analysis

Facial movement during 2P calcium imaging was recorded using an infrared camera (FLIR, Flea3 USB3 combined with a Tamron 12VM412ASIR 1/2" 4-12mm F/1.2 Infrared Manual C-Mount Lens) triggered by 2P image acquisition at around 15.5 Hz. Video files were further processed using Facemap[47] and Matlab. Here the motion energy was extracted from a manually drawn region of interest around the whisker pad.

Z-scored whisker energy was calculated using the 2 to 0 seconds before tone onset per trial. The peak of the Z-scored whisker energy was extracted between 0 and 0.5 s and averaged across trials for analysis in Fig S1. Trials were removed from pure-tone analysis if the mean Z-scored whisker energy in either 0.5 s after tone onset or offset was above 2.

Two-photon calcium imaging analysis

Raw images were pre-processed using the SpecSeg toolbox[48] to select regions of interest (ROIs) that correspond to the soma's of neurons and extract the mean fluorescence signal. In brief, first, rigid motion corrected was performed using NoRMCorre[49], then ROIs were selected based on cross-spectral power across pixels. ROIs were manually refined, and mean signal was extracted per ROI. Then, neuropil was subtracted subtracting 70% of the average pixel values around from a doughnut around the ROI. ΔF/F Values were calculated by subtraction of moving baseline and then dividing by a linear fit of that moving baseline (10th percentile over 500 frames).

To increase the temporal resolution of the ΔF/F trace we used a spike deconvolution algorithm (MLspike, autocalibration of parameters per neuron)[35]. Additionally, run speed was regressed out of the estimated spike times using a linear model ('fitlm' in Matlab). The residual estimation of the firing rate (FR) was used to calculate the ΔFR by subtracting the mean activity 0.5 to 1 s from before tone onset.

bioRxiv preprint doi: https://doi.org/10.1101/2024.08.31.610645; this version posted September 5, 2024. The copyright holder for this preprint (which was not certified by peer review) is the author/funder, who has granted bioRxiv a license to display the preprint in perpetuity. It is made available under aCC-BY-NC 4.0 International license.

After removal of whisker movement trials, responses to pure-tone stimuli were calculated by taking the trial-averaged ΔFR 0 to 0.5 s after tone onset and offset or 0 to 0.5 s after drifting grating onset. A minimum of trials per tone was set at 8 after removal of trials, otherwise the tone was ignored for further analysis. For calculation of response type and response amplitude the period (after tone onset or offset for pure tones or just after grating onset) with the largest significant response was taken from the stimuli with the strongest significant response (best frequency for pure-tone stimuli or preferred stimulus for drifting gratings). A neuron was deemed significantly responding if the ΔFR response from at least one stimulus type exceeded a trial-shuffled threshold. The threshold was set as the 0.1st percentile of a 1000 times shuffled distribution of ΔFR response amplitudes, where the deconvolved spike time were circularly shifted by a random time every shuffle.

Linear discriminant analysis

For population decoding analysis a linear discriminant analysis classifier ('fitcdiscr' in Matlab with 0 gamma correction) was trained to predict trial types based on the $\Delta F/F_0$ signal. The $\Delta F/F_0$ signal was calculated by subtracting the mean ΔF/F signal over 1 to 0 seconds before stimulus onset from the mean ΔF/F signal over 0.2 to 1.2 s after stimulus onset. From the $\Delta F/F_0$ response Z-scored whisker energy (for pure-tone stimuli only) and run speed were regressed out using 'fitlm' in Matlab. These residual $\Delta F/F_0$ were used as predictors in the decoding model and sound intensity, sound frequency, grating direction or grating contrast as labels. The number of neurons used were randomly drawn and limited to the smallest size across groups tested. The prediction accuracy was calculated and validated using 5-fold cross validation. These procedures were repeated 100 times to produce a distribution of prediction accuracies. Performance above chance was tested with a label-shuffled distribution with similar analysis. Significance (above chance and between groups) was tested using a permutation test with 100000 iterations.

Statistical analysis

Statistical details are written in the figure legends. For two-way ANOVAs and repeated measures ANOVAs the data was assumed to be normally distributed. Repeated measures two-way ANOVAs were Geisser-Greenhouse corrected. Data is plotted as mean ± SEM, except for LDA data which is plotted as mean ± SD.

bioRxiv preprint doi: https://doi.org/10.1101/2024.08.31.610645; this version posted September 5, 2024. The copyright holder for this preprint (which was not certified by peer review) is the author/funder, who has granted bioRxiv a license to display the preprint in perpetuity. It is made available under aCC-BY-NC 4.0 International license.

ANOVAs and Fisher's exact tests were performed in Graphpad Prism 10 and Mann-Whitney U tests and permutations tests in Matlab (R2023b).

ACKNOWLEDGEMENTS

We wish to thank the Levelt lab for helpful discussion, the members of the mechatronics department for technical support and animal caretaker of the Netherlands Institute for Neuroscience for their help. We thank Vasileios Patsourakos, Maaike van der Aa and Ayana Kemble for help with habituation of the mice and Chris van der Togt, Matthew W. Self, Pieter W. Roelfsema and Gerard Borst for technical support, data analysis and data management support. This project received funding from the European Union's Horizon 2020 Research and Innovation Program under grant agreement nos. 785907 (HBP SGA2, CL & PR) and 945539 (HBP SGA3, CL & PR) and the Dutch Research Council (FlagEra SoundSight, 680-91-320, CL). The authors declare that they have no competing interests.

LITERATURE

1. Sabourin, C.J., Merrikhi, Y., and Lomber, S.G. (2022). Do blind people hear better? Trends Cogn. Sci. *26*, 999–1012.

2. Fine, I., and Park, J.M. (2018). Blindness and human brain plasticity. Annu. Rev. Vis. Sci. *4*, 337–356.

3. Collignon, O., Vandewalle, G., Voss, P., Albouy, G., Charbonneau, G., Lassonde, M., and Lepore, F. (2011). Functional specialization for auditory-spatial processing in the occipital cortex of congenitally blind humans. Proc. Natl. Acad. Sci. U. S. A. *108*, 4435–4440.

4. Merabet, L.B., and Pascual-Leone, A. (2010). Neural reorganization following sensory loss: The opportunity of change. Nat. Rev. Neurosci. *11*, 44–52.

5. Gougoux, F., Lepore, F., Lassonde, M. et al (2004). Pith discrimination in the early blind. Nature *430*.

6. Mowad, T.G., Willett, A.E., Mahmoudian, M., Lipin, M., Heinecke, A., Maguire, A.M., Bennett, J., and Ashtari, M. (2020). Compensatory Cross-Modal Plasticity Persists After Sight Restoration. Front. Neurosci. *14*, 1–16.

7. Dormal, G., Lepore, F., Harissi-Dagher, M., Albouy, G., Bertone, A., Rossion, B., and Collignon, O. (2015). Tracking the evolution of crossmodal plasticity and visual functions before and after sight restoration. J. Neurophysiol. *113*, 1727–1742.

8. Fine, I., Wade, A.R., Brewer, A.A., May, M.G., Goodman, D.F., Boynton, G.M., Wandell, B.A., and MacLeod, D.I.A. (2003). Long-term deprivation affects visual perception and cortex. Nat. Neurosci. *6*, 915–916.

bioRxiv preprint doi: https://doi.org/10.1101/2024.08.31.610645; this version posted September 5, 2024. The copyright holder for this preprint (which was not certified by peer review) is the author/funder, who has granted bioRxiv a license to display the preprint in perpetuity. It is made available under aCC-BY-NC 4.0 International license.

9. Saenz, M., Lewis, L.B., Huth, A.G., Fine, I., and Koch, C. (2008). Visual motion area MT + /V5 responds to auditory motion in human sight-recovery subjects. J. Neurosci. *28*, 5141–5148.

10. Bennett, C.R., Bauer, C.M., Bailin, E.S., and Merabet, L.B. (2020). Neuroplasticity in cerebral visual impairment (CVI): Assessing functional vision and the neurophysiological correlates of dorsal stream dysfunction. Neurosci. Biobehav. Rev. *108*, 171–181.

11. Smith, I.T., Townsend, L.B., Huh, R., Zhu, H., and Smith, S.L. (2017). Stream-dependent development of higher visual cortical areas. Nat. Neurosci. *20*, 200–208.

12. Kowalewski, N.N., Kauttonen, J., Stan, P.L., Jeon, B.B., Fuchs, T., Chase, S.M., Lee, T.S., and Kuhlman, S.J. (2020). Development of Natural Scene Representation in Primary Visual Cortex Requires Early Postnatal Experience. Curr. Biol., 1–12.

13. Dahlhaus, M., Li, K.W., Van Der Schors, R.C., Saiepour, M.H., Van Nierop, P., Heimel, J.A., Hermans, J.M., Loos, M., Smit, A.B., and Levelt, C.N. (2011). The synaptic proteome during development and plasticity of the mouse visual cortex. Mol. Cell. Proteomics *10*, M110.005413.

14. Cheng, S., Butrus, S., Tan, L., Xu, R., Sagireddy, S., Trachtenberg, J.T., Shekhar, K., and Zipursky, S.L. (2022). Vision-dependent specification of cell types and function in the developing cortex. Cell *185*, 311-327.e24.

15. Chen, X., Fischer, S., Rue, M.C.P., Zhang, A., Mukherjee, D., Kanold, P.O., Gillis, J., and Zador, A.M. (2024). Whole-cortex in situ sequencing reveals input-dependent area identity. Nature.

16. Deneux, T., Kempf, A., and Bathellier, B. (2019). Context-dependent signaling of coincident auditory and visual events in primary visual cortex. Elife, 258970.

17. Iurilli, G., Ghezzi, D., Olcese, U., Lassi, G., Nazzaro, C., Tonini, R., Tucci, V., Benfenati, F., and Medini, P. (2012). Sound-Driven Synaptic Inhibition in Primary Visual Cortex. Neuron *73*, 814–828.

18. Meijer, G.T., Marchesi, P., Mejias, J.F., Montijn, J.S., Lansink, C.S., and Pennartz, C.M.A. (2020). Neural Correlates of Multisensory Detection Behavior: Comparison of Primary and Higher-Order Visual Cortex. Cell Rep. *31*, 107636.

19. Meijer, G.T., Montijn, J.S., Pennartz, C.M.A., and Lansink, C.S. (2017). Audiovisual modulation in mouse primary visual cortex depends on cross-modal stimulus configuration and congruency. J. Neurosci. *37*, 8783–8796.

20. Meijer, G.T., Mertens, P.E.C., Pennartz, C.M.A., Olcese, U., and Lansink, C.S. (2019). The circuit architecture of cortical multisensory processing: Distinct functions jointly operating within a common anatomical network. Prog. Neurobiol. *174*, 1–15.

21. Williams, A.M., Angeloni, C.F., and Geffen, M.N. (2023). Sound Improves Neuronal Encoding of Visual Stimuli in Mouse Primary Visual Cortex. J. Neurosci. *43*, 2885–2906.

22. Mazo, C., Baeta, M., and Petreanu, L. (2024). Auditory cortex conveys non-topographic sound localization signals to visual cortex. Nat. Commun. *15*, 1–16.

23. Piché, M., Chabot, N., Bronchti, G., Miceli, D., Lepore, F., and Guillemot, J.P. (2007). Auditory responses in the visual cortex of neonatally enucleated rats. Neuroscience *145*, 1144–1156.

24. Izraeli, R., Koay, G., Lamish, M., Heicklen-Klein, A.J., Heffner, H.E., Heffner, R.S., and Wollberg, Z. (2002). Cross-modal neuroplasticity in neonatally enucleated hamsters: Structure, electrophysiology and behaviour. Eur. J. Neurosci. *15*, 693–712.

25. Laemle, L.K., Strominger, N.L., and Carpenter, D.O. (2006). Cross-modal innervation of primary visual cortex by auditory fibers in congenitally anophthalmic mice. Neurosci. Lett. *396*, 108–112.

26. Oude Lohuis, M.N., Marchesi, P., Olcese, U., and Pennartz, C.M.A. (2024). Triple dissociation of visual, auditory and motor processing in mouse primary visual cortex. Nat. Neurosci. *27*,

bioRxiv preprint doi: https://doi.org/10.1101/2024.08.31.610645; this version posted September 5, 2024. The copyright holder for this preprint (which was not certified by peer review) is the author/funder, who has granted bioRxiv a license to display the preprint in perpetuity. It is made available under aCC-BY-NC 4.0 International license.

758–771.

27. Bimbard, C., Sit, T.P.H., Lebedeva, A., Reddy, C.B., Harris, K.D., and Carandini, M. (2023). Behavioral origin of sound-evoked activity in mouse visual cortex. Nat. Neurosci. *26*, 251–258.

28. Marshel, J.H., Garrett, M.E., Nauhaus, I., and Callaway, E.M. (2011). Functional specialization of seven mouse visual cortical areas. Neuron *72*, 1040–1054.

29. van Beest, E.H., Mukherjee, S., Kirchberger, L., Schnabel, U.H., van der Togt, C., Teeuwen, R.R.M., Barsegyan, A., Meyer, A.F., Poort, J., Roelfsema, P.R., et al. (2021). Mouse visual cortex contains a region of enhanced spatial resolution. Nat. Commun. *12*.

30. Garrett, M.E., Nauhaus, I., Marshel, J.H., Callaway, E.M., Garrett, M.E., Marshel, J.H., Nauhaus, I., and Garrett, M.E. (2014). Topography and areal organization of mouse visual cortex. J. Neurosci. *34*, 12587–12600.

31. Glickfeld, L.L., and Olsen, S.R. (2017). Higher-Order Areas of the Mouse Visual Cortex. Annu. Rev. Vis. Sci. *3*, 251–273.

32. Wang, Q., Ding, S.L., Li, Y., Royall, J., Feng, D., Lesnar, P., Graddis, N., Naeemi, M., Facer, B., Ho, A., et al. (2020). The Allen Mouse Brain Common Coordinate Framework: A 3D Reference Atlas. Cell *181*, 936-953.e20.

33. Clayton, K.K., Stecyk, K.S., Guo, A.A., Chambers, A.R., Chen, K., Hancock, K.E., and Polley, D.B. (2024). Sound elicits stereotyped facial movements that provide a sensitive index of hearing abilities in mice. Curr. Biol. *34*, 1605-1620.e5.

34. Park, C.R., Willott, J.F., and Walton, J.P. (2024). Age-related changes of auditory sensitivity across the life span of CBA/CaJ mice. Hear. Res. *441*, 108921.

35. Deneux, T., Kaszas, A., Szalay, G., Katona, G., Lakner, T., Grinvald, A., Rozsa, B., and Vanzetta, I. (2016). Accurate spike estimation from noisy calcium signals for ultrafast three-dimensional imaging of large neuronal populations in vivo. Nat. Commun. *7*.

36. Bowen, Z., Winkowski, D.E., and Kanold, P.O. (2020). Functional organization of mouse primary auditory cortex in adult C57BL/6 and F1 (CBAxC57) mice. Sci. Rep. *10*, 1–14.

37. Atkinson, J. (2017). The davida teller award lecture, 2016 visual brain development: A review of “dorsal stream vulnerability”-motion, mathematics, amblyopia, actions, and attention. J. Vis. *17*, 1–24.

38. Collignon, O., Dormal, G., De Heering, A., Lepore, F., Lewis, T.L., and Maurer, D. (2015). Long-Lasting Crossmodal Cortical Reorganization Triggered by Brief Postnatal Visual Deprivation. Curr. Biol. *25*, 2379–2383.

39. Bimbard, C., Sit, T.P.H., Lebedeva, A., Reddy, C.B., Harris, K.D., and Carandini, M. (2023). Behavioral origin of sound-evoked activity in mouse visual cortex. Nat. Neurosci. *26*, 251–258.

40. De León Reyes, N.S., Mederos, S., Varela, I., Weiss, L.A., Perea, G., Galazo, M.J., and Nieto, M. (2019). Transient callosal projections of L4 neurons are eliminated for the acquisition of local connectivity. Nat. Commun. *10*, 1–15.

41. Charbonneau, V., Laramée, M.E., Boucher, V., Bronchti, G., and Boire, D. (2012). Cortical and subcortical projections to primary visual cortex in anophthalmic, enucleated and sighted mice. Eur. J. Neurosci. *36*, 2949–2963.

42. Karlen, S.J., Kahn, D.M., and Krubitzer, L. (2006). Early blindness results in abnormal corticocortical and thalamocortical connections. Neuroscience *142*, 843–858.

43. de Heering, A., Dormal, G., Pelland, M., Lewis, T., Maurer, D., and Collignon, O. (2016). A Brief Period of Postnatal Visual Deprivation Alters the Balance between Auditory and Visual Attention. Curr. Biol. *26*, 3101–3105.

44. Chabot, N., Charbonneau, V., Laramée, M.E., Tremblay, R., Boire, D., and Bronchti, G. (2008). Subcortical auditory input to the primary visual cortex in anophthalmic mice. Neurosci. Lett. *433*, 129–134.

bioRxiv preprint doi: https://doi.org/10.1101/2024.08.31.610645; this version posted September 5, 2024. The copyright holder for this preprint (which was not certified by peer review) is the author/funder, who has granted bioRxiv a license to display the preprint in perpetuity. It is made available under aCC-BY-NC 4.0 International license.

45. Daigle, T.L., Madisen, L., Hage, T.A., Valley, M.T., Knoblich, U., Larsen, R.S., Takeno, M.M., Huang, L., Gu, H., Larsen, R., et al. (2018). A Suite of Transgenic Driver and Reporter Mouse Lines with Enhanced Brain-Cell-Type Targeting and Functionality. Cell *174*, 465-480.e22.

46. Zhang, Y., Rózsa, M., Liang, Y., Bushey, D., Wei, Z., Zheng, J., Reep, D., Broussard, G.J., Tsang, A., Tsegaye, G., et al. (2023). Fast and sensitive GCaMP calcium indicators for imaging neural populations. Nature *615*, 884–891.

47. Syeda, A., Zhong, L., Tung, R., Long, W., Pachitariu, M., and Stringer, C. (2024). Facemap: a framework for modeling neural activity based on orofacial tracking. Nat. Neurosci. *27*, 187–195.

48. de Kraker, L., Seignette, K., Thamizharasu, P., van den Boom, B.J.G., Pica, I.F., Willuhn, I., Levelt, C.N., and van der Togt, C. (2021). SpecSeg: cross spectral power-based segmentation of neurons and neurites in chronic calcium imaging datasets.

49. Pnevmatikakis, E.A., and Giovannucci, A. (2017). NoRMCorre: An online algorithm for piecewise rigid motion correction of calcium imaging data. J. Neurosci. Methods *291*, 83–94.